

Differential timing of gene expression and recruitment in independent origins of CAM in the Agavoideae (Asparagaceae)

Karolina Heyduk^{1,2,3} , Edward V. McAssey¹  and Jim Leebens-Mack² 

¹School of Life Sciences, University of Hawai'i at Mānoa, Honolulu, HI 96822, USA; ²Department of Plant Biology, University of Georgia, Athens, GA 30602, USA; ³Department of Ecology and Evolutionary Biology, Yale University, New Haven, CT 06520, USA

Summary

Author for correspondence:
Karolina Heyduk
Email: heyduk@hawaii.edu

Received: 1 December 2021
Accepted: 9 May 2022

New Phytologist (2022) **235**: 2111–2126
doi: 10.1111/nph.18267

Key words: Agavoideae, carboxylation, Crassulacean acid metabolism photosynthesis, comparative transcriptomics, *Yucca*.

- Crassulacean acid metabolism (CAM) photosynthesis has evolved repeatedly across the plant tree of life, however our understanding of the genetic convergence across independent origins remains hampered by the lack of comparative studies. Here, we explore gene expression profiles in eight species from the Agavoideae (Asparagaceae) encompassing three independent origins of CAM.
- Using comparative physiology and transcriptomics, we examined the variable modes of CAM in this subfamily and the changes in gene expression across time of day and between well watered and drought-stressed treatments. We further assessed gene expression and the molecular evolution of genes encoding phosphoenolpyruvate carboxylase (PPC), an enzyme required for primary carbon fixation in CAM.
- Most time-of-day expression profiles are largely conserved across all eight species and suggest that large perturbations to the central clock are not required for CAM evolution. By contrast, transcriptional response to drought is highly lineage specific. *Yucca* and *Beschorneria* have CAM-like expression of *PPC2*, a copy of *PPC* that has never been shown to be recruited for CAM in angiosperms.
- Together the physiological and transcriptomic comparison of closely related C₃ and CAM species reveals similar gene expression profiles, with the notable exception of differential recruitment of carboxylase enzymes for CAM function.

Introduction

The repeated origin of phenotypes across the tree of life has long fascinated biologists, particularly in cases in which such phenotypes are assembled convergently, that is, using the same genetic building blocks. Documented examples of convergent evolution in which the same genetic mechanisms are involved include the repeated origins of betalain pigmentation in the Caryophyllales (Sheehan *et al.*, 2020), the origins of caffeine biosynthesis in eudicots (Denoeud *et al.*, 2014), and the multiple transitions to red flowers in *Ipomoea* (Streisfeld & Rausher, 2009), among others. In all these cases, careful analysis of the genetic components underlying the repeated phenotypic evolution was driven by recruitment or loss of function of orthologous genes. Such convergence in the genetic mechanism suggests that the evolutionary path toward these phenotypes is relatively narrow, meaning the phenotype can only be obtained through a small set of very important molecular changes.

Such shared molecular mechanisms of repeated phenotypic evolution are especially surprising when observed across larger clades. For example, across all flowering plants, the large number of independent origins (*c.* 100) of both C₄ and

Crassulacean acid metabolism (CAM) photosynthesis imply relatively straightforward genetic and evolutionary paths from the ancestral C₃ photosynthetic pathway (Edwards, 2019; Heyduk *et al.*, 2019a). The overall photosynthetic metabolic pathway in C₄ and CAM species is largely conserved; CO₂ is converted to a four carbon acid by phosphoenolpyruvate carboxylase (PPC) and either moved to adjoining cells (C₄) or stored in the vacuole overnight (CAM). The four carbon acids are then decarboxylated, resulting in high concentrations of CO₂ in the cells in which Rubisco is active. Although some aspects of these photosynthetic pathways can vary among independent lineages, such as decarboxylation pathways in C₄ lineages (Christin *et al.*, 2009; Bräutigam *et al.*, 2014), the same homologue of some genes has been repeatedly recruited for carbon concentration. In three independently derived C₄ grass lineages, five out of seven photosynthetic genes examined had the same gene copy (orthologues) recruited, despite the presence of alternative copies (paralogues) of each gene (Christin *et al.*, 2013). In *Cleome gynandra* (Cleomaceae) and *Zea mays* (Poaceae), transcription factors that induce expression of C₄ photosynthetic genes in the required cell-specific manner were orthologous, despite >140 million years (Myr) of evolution separating the two lineages (Aubry *et al.*, 2014).

While C_4 is known for the unique Kranz anatomy that allows the carbon concentrating mechanism to function efficiently, CAM instead relies on the temporal separation of CO_2 assimilation and conversion of CO_2 into sugars. The diurnal cycle of primary CO_2 fixation and photosynthesis in CAM plants is thought to require a close integration with the circadian clock, although how that is explicitly accomplished remains unknown. Studies have shown that only a handful of core clock genes differ in their expression between C_3 and CAM species (Yang *et al.*, 2017; Yin *et al.*, 2018), although many of these studies have relied on comparisons of distantly related species, confounding changes attributable to evolutionary distance with those that underlie the evolution of CAM photosynthesis. While the core clock seems largely similar in CAM and C_3 species, 24-h expression profiles for genes involved in carboxylation, decarboxylation, sugar metabolism, and stomatal movement have been shown to differ between C_3 and CAM species (Ceusters *et al.*, 2014; Ming *et al.*, 2015; Abraham *et al.*, 2016; Heyduk *et al.*, 2018a; Wai *et al.*, 2019), suggesting a regulatory link between clock genes and genes contributing to CAM function.

A hallmark of CAM is the evening expression of phosphoenolpyruvate carboxylase (PPC) genes, which produce the enzyme required for the initial fixation of atmospheric CO_2 into an organic acid in both C_4 and CAM plants. Unlike Rubisco, which has affinities for both CO_2 and O_2 , PPC has only carboxylase function, which it uses to convert bicarbonate and phosphoenolpyruvate (PEP) into oxaloacetate (OAA). The carboxylating function of PPC is used by all plants to supplement intermediate metabolites into the tricarboxylic acid (TCA) cycle, and therefore PPC genes are present in all plant lineages in multiple copies. Phosphoenolpyruvate carboxylase enzymes used by the CAM pathway are active in the evening and night, whereas TCA-related PPC enzymes are likely to have constitutive expression across the diel cycle, with perhaps higher activity during the day. Transcriptomic investigations of CAM species have shown that expression of the PPC genes involved in CAM is induced to much higher levels at dusk and overnight (Ming *et al.*, 2015; Brilhous *et al.*, 2016; Yang *et al.*, 2017; Heyduk *et al.*, 2018a, 2019b): expression levels of CAM PPCs can be 100–1000× higher than PPC homologues contributing to housekeeping functions.

There are two main families of PPC genes in flowering plants: *PPC1*, which is typically present in 2–6 copies in most lineages (Deng *et al.*, 2016), and *PPC2*, which shares homology with a PPC gene copy found in bacteria, and is typically found in single or low copy in plant genomes. *PPC1* forms a homotetramer, whereas *PPC2* requires the formation of a hetero-octamer with *PPC1* to function (O'Leary *et al.*, 2009). *PPC1* is used in the TCA cycle in plants, and in all published cases within angiosperms a *PPC1* gene copy is recruited for CAM (and C_4) function. New work in the lycophyte *Isoetes taiwanensis* has shown novel recruitment of *PPC2* into the CAM pathway, rather than *PPC1* (Wickell *et al.*, 2021). *PPC2* has been shown to be involved in pollen maturation, fatty acid production in seeds, and possibly root development and salt sensing (Gennidakis *et al.*, 2007; Igawa *et al.*, 2010; Wang *et al.*, 2012), although overall consensus on *PPC2* function in plants remains elusive.

To understand both the evolution of CAM, as well as the recruitment of *PPC* homologues in independent origins of CAM, we built upon existing physiological and transcriptomic data in the Agavoideae (Asparagaceae) by investigating additional species. Crassulacean acid metabolism has evolved three times independently in the Agavoideae (Fig. 1): once in *Agave* *sensu lato* (*Agave* s.l., includes the genera *Agave*, *Manfreda*, and *Polianthes*), once in *Yucca*, and once in *Hesperaloe* (Heyduk *et al.*, 2016b). Previous research compared gene expression and physiology in closely related C_3 and CAM *Yucca* species (Heyduk *et al.*, 2019b) and, separately, in species that ranged from weak CAM (low amounts of nocturnal CO_2 uptake) to strong CAM in *Agave* s.l. (Heyduk *et al.*, 2018b). Gene expression profiles for key CAM genes in the C_3 *Yucca* species studies showed CAM-like expression, especially when drought stressed, suggesting that perhaps *Yucca* or even the Agavoideae as a whole was primed for the evolution of CAM due to gene regulatory networks and expression patterns that existed in a C_3 ancestor. Here we conducted additional RNA sequencing in two species of *Hesperaloe* (CAM) and one species of *Hosta* (C_3) to assess (1) how gene expression varies in timing of expression and in response to drought stress across Agavoideae and (2) to what extent have the three independent origins of CAM in the Agavoideae been involved in recruitment of the same carboxylating enzyme gene homologues.

Materials and Methods

Plant growth and physiological sampling

Plants of *Hesperaloe parviflora* (accession: PARL 436) and *Hesperaloe nocturna* (accession: PARL 435) were grown from seed acquired in 2014 from the USDA Germplasm Resources Information Network (GRIN). *Hesperaloe* plants were kept in the

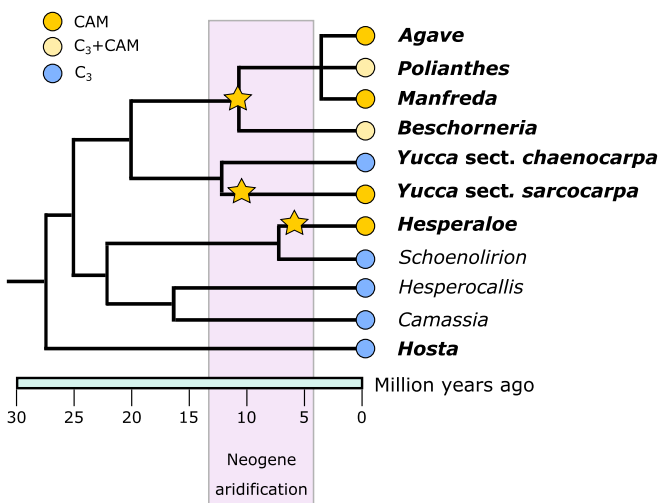


Fig. 1 Simplified phylogeny of the Agavoideae, with estimated topology and mean divergence times from McKain *et al.* (2016), and aridification timing based on Eronen *et al.* (2012). Bolded taxa names are the species/genera included in this study. Tips are labelled according to photosynthetic pathway as described by previous work (Heyduk *et al.*, 2016b, 2018b, 2019b), and yellow stars indicate hypothesised origins of Crassulacean acid metabolism photosynthesis.

University of Georgia (UGA) Plant Biology glasshouses with once weekly watering. *Hosta* plants were purchased for New Hampshire Hostas (<https://www.nhhostas.com/>) in January 2018 and kept on a misting bench at the same glasshouses until experimentation began in March 2018. Replicates of each species ($n = 4$, 4 and 6 for *H. parviflora*, *H. nocturna*, and *H. venusta*, respectively) were placed into a walk-in Conviron growth chamber, with day length set to 12 h (lights on at 7:00 h), day : night temperatures 30 : 17°C, humidity at 30%, and maximum PAR (*c.* 400 $\mu\text{mol m}^{-2} \text{s}^{-1}$ at plant level).

Plants were acclimated in the growth chamber for 4 d before sampling and watered to saturation daily. On day 1, plants were sampled every 2 h, beginning at 1 h after the lights were turned on, for gas exchange using a Li-Cor 6400XT. Due to the small size of the plants, only two replicates of *Hosta* had Li-Cor measurements taken; one replicate of *Hesperaloe nocturna* was not measured due to an ant infestation in the pot. After day 1, water was withheld for 5 d in all plants with the exception of *Hosta*, which were all removed from the experiment at this point. On day 7, all the remaining plants' water status had dropped to 8% soil water content, and plants were measured again for gas exchange. After day 7, plants were re-watered and one more day of gas exchange sampling was conducted on day 9. Triplicate leaf tissue samples per plant were collected for titratable acidity measurements 2 h before lights turned on (pre-dawn sample) and 2 h before lights turned off (pre-dusk sample) on days 1 and 7. Samples for leaf titrations were immediately flash frozen and stored at -80°C .

Leaf acid titrations were conducted as in Heyduk *et al.* (2018b); briefly, frozen leaf discs were quickly weighed and placed into 60 ml of 20% EtOH. Samples were boiled until the volume was reduced to half, then 30 ml of diH₂O was added. Samples were reduced to half again and a final volume of 30 ml of diH₂O was added. Samples were allowed to cool then titrated to pH 7.0 using 0.002 M NaOH. Total micromoles H⁺ per gram of frozen mass was calculated as ($\text{ml NaOH} \times 0.002 \text{ M}$) g⁻¹. Pre-dusk values were subtracted from pre-dawn values to determine the change, or ΔH^+ , per replicate. All statistical analyses were conducted in R v.3.5.0 (R Core Team, 2021). Physiology data for *Agave*, *Polianthes*, *Beschorneria*, and *Yucca* species were taken from previously published data (Heyduk *et al.*, 2016a, 2018b); for comparison, we include soil moisture data as measured from the three independent studies during the drought stress (Supporting Information Table S1).

RNA sequencing and assembly

Tissue for RNA sequencing was collected every 4 h from each of the three species, from four replicate plants per species. For *H. nocturna* and *H. parviflora*, samples were collected from both well watered and drought-stressed plants (days 1 and 7). For *H. venusta*, only well watered samples were collected. Tissue was flash frozen in N₂, then stored at -80°C . RNA was isolated using a Qiagen RNeasy Plant Kit, purified with Ambion Turbo DNase, and quantified by a NanoDrop spectrophotometer and

Agilent Bioanalyzer v.2100 (Santa Clara, CA, USA). RNA-sequencing libraries were constructed with a KAPA Stranded RNA-seq kit at half reaction volume and barcoded separately using dual barcodes (Glenn *et al.*, 2019). Library concentrations were measured by quantitative PCR, pooled in sets of 28–29 libraries, and sequenced with PE 75 bp reads on an Illumina NextSeq system at the Georgia Genomics and Bioinformatics Core at the University of Georgia. Raw reads from sequencing *Hesperaloe* and *Hosta* species are available on the NCBI Sequence Read Archive (SRA), under BioProject PRJNA755802.

Raw reads were processed with TRIMOMATIC v.0.36 (Bolger *et al.*, 2014) and paired reads were assembled *de novo* for each of the three species (*H. parviflora*, *H. nocturna*, and *Hosta venusta*) in TRINITY v.2.5.1 (Grabherr *et al.*, 2011). Reads were initially mapped to the entire TRINITY-assembled transcriptome for each species with BOWTIE v.2.0 (Langmead & Salzberg, 2012). TRINITY 'isoforms' that had < 2 transcripts mapped per million (TPM) abundance, or constituted $< 20\%$ of total component expression, were removed. Transcriptome assemblies of sister species, including *Agave bracteosa*, *Polianthes tuberosa*, and *Beschorneria yuccoides* (Heyduk *et al.*, 2018b) had already been filtered by the same thresholds as above. All six filtered assemblies had open reading frames (ORFs) predicted by TRANSDECODER v.2.1 (Grabherr *et al.*, 2011) using both 'LongOrfs' and 'Predict' functions and keeping only the best scoring ORF per transcript.

To sort the predicted TRANSDECODER sequences into gene families, we generated orthogroups circumscribed from nine reference genomes downloaded from the PHYTOZOME portal (Goodstein *et al.*, 2012), with a particular focus on monocots. Translated primary transcript sequences were downloaded for *Acorus americanus* v.1.1 (DOE-JGI, <http://phytozome-next.jgi.doe.gov/>), *Arabidopsis thaliana* v.Araport11 (Cheng *et al.*, 2017), *Asparagus officinalis* v.1.1 (Harkess *et al.*, 2017), *Ananas comosus* v.3 (Ming *et al.*, 2015), *Amborella trichopoda* v.1 (Amborella Genome Project, 2013), *Brachypodium distachyon* v.3.1 (International Brachypodium Initiative, 2010), *Dioscorea alata* v.2.1 (Bredeson *et al.*, 2022), *Musa acuminata* v.1 (D'Hont *et al.*, 2012), *Oryza sativa* v.7 (Ouyang *et al.*, 2007), *Sorghum bicolor* v.3.1.1 (McCormick *et al.*, 2018), and *Setaria italica* v.2.2 (Bennetzen *et al.*, 2012) from PHYTOZOME. Translated coding sequences from these genomes were clustered using ORTHOFINDER v.2.2.7 (Emms & Kelly, 2019). In addition to the above published genomes, preliminary draft genome annotations (primary translated transcripts) for *Yucca aloifolia* and *Yucca filamentosa* were secondarily added to the orthogroup analyses using the -b flag of ORTHOFINDER (pre-publication permission from JGI was obtained for *Yucca* annotation use). Finally, TRANSDECODER translated coding sequences for the Agavoideae species were then added to the orthogroup circumscription again using the -b flag.

Expression analysis

Reads were remapped using KALLISTO (Bray *et al.*, 2016) onto the filtered transcriptomes (iso_pct > 20, TPM > 2, TRANSDECODER best scoring ORF) for the *de novo* assemblies of *Hesperaloe* and *Hosta*. For the two *Yucca* genomes, existing RNA-seq reads (from

Heyduk *et al.*, 2019b) were mapped onto the annotated primary transcripts using KALLISTO. Because previously published expression analysis of *Agave*, *Beschorneria*, and *Polianthes* was done on transcriptomes filtered the same way (iso_pct > 20, TPM > 2) (Heyduk *et al.*, 2018b), expression data in the form of read counts and TPM values for genes were used as previously published. Count and TPM matrices for all taxa analysed here, as well as orthogroup annotations, are available on github (www.github.com/kheyduk/AgavoideaeComparative).

Read counts for the two *Hesperaloe* species, *Hosta*, and the two *Yucca* species were imported into R for initial outlier filtering in EDGER (Robinson *et al.*, 2010) and subsequent time-structured expression analysis in MASIGPRO (Cenesa *et al.*, 2006; Nueda *et al.*, 2014). The latter program fits read count data to regressions, taking into account treatments (well watered and drought stress), and asks whether a polynomial regression of degree n (chosen to be 5, or one less the number of timepoints) is a better fit to each gene than a straight line. Genes with expression patterns across time can be best explained by a polynomial regression are from this point forwards referred to as 'time structured'. While read counts are required for the MASIGPRO analysis, all comparative expression plots presented use TPM normalised expression. Time-structured expression information for *Agave*, *Beschorneria*, and *Polianthes* was taken from previously published data (Heyduk *et al.*, 2018b).

Circadian gene expression

Previous studies in CAM have shown that a few circadian regulators get re-wired in the evolution of CAM (Moseley *et al.*, 2018; Wai *et al.*, 2019). To determine whether these patterns held in more closely related C₃ and CAM species, the expression of circadian clock genes was compared between members of the Agavoideae. From the list of genes that had significantly time-structured expression from MASIGPRO for each species, we assessed gene family presence/absence data from the ORTHOFINDER gene circumscriptions. Shared gene family presence in the time-structured expression was assessed using the UpSETR package (Conway *et al.*, 2017) in R 4.0.4 (R Core Team, 2021). A curated list of *Arabidopsis thaliana* circadian genes was used to examine the extent to which time-structured expression of circadian genes was shared across all eight species. Finally, for circadian-annotated genes, we used JTK_CYCLE (Hughes *et al.*, 2010) and LOMB-SCARGLE (Glynn *et al.*, 2005) methods implemented in METACYCLE (Wu *et al.*, 2016) to obtain period, lag and amplitude for genes with a period expression pattern. Cycling patterns for *Agave* and *Beschorneria* were excluded from further analysis, as their resolution (number of replicates and time points) was lower than other species due to dropped libraries (Heyduk *et al.*, 2018b). We then used ANOVA to assess whether there were differences in average phase across ORTHOFINDER gene families between CAM and C₃ species, as well as between *Hosta* and the other Agavoideae species. *P*-values were corrected for multiple testing using the Benjamini–Hochberg correction.

PPC evolution

The *PPC1* and *PPC2* gene families were identified in the ORTHOFINDER-circumscribed orthogroups by searching for annotated *Arabidopsis* *PPC1* and *PPC2* copies. Both orthogroups were manually inspected for completeness by checking if all known genes from sequenced and annotated genomes were properly sorted into those two orthogroups. Only sequences that were at least 50% of the length of the longest sequence (based on coding sequence) were retained and aligned. Because *de novo* transcriptomes often contain allelic variation assembled as separate contigs, we developed a threshold to collapse highly similar sequences within a species. Using gene annotations from the two *Yucca* species, we calculated pairwise sequence similarities within each species by gene combination (*PPC1* or *PPC2*). The highest similarity within a gene was used as a cutoff; it represented the highest sequence similarity that existed within a species across separate gene copies. Because the *Yucca* annotation is based on genomic sequence, we felt confident that separate assembled genes represented loci, rather than alleles. The highest within-species similarity in *Yucca* for *PPC1* was 96.23% and 99.71% for *PPC2*. Sequences from the *de novo* transcriptomes were then collapsed within a species if they were more similar than these percentages; instead of using ambiguity codes, we used the longest sequence as the representative for the collapsed sequences. To get in-frame coding sequence alignment, each orthogroup protein and CDS output from TRANSDECODER was used to align the coding sequences using PAL2NAL (Suyama *et al.*, 2006). Phylogenetic trees for *PPC1* and *PPC2* were estimated on the in-frame coding sequence alignments using IQTREE v.2.0 Nguyen *et al.*, 2015; Minh *et al.*, 2020 and 1000 rapid bootstrap replicates, using built-in MODELINDER to determine the best substitution model. The resulting tree for each gene family, along with the in-frame coding sequence alignment, were used to estimate shifts in molecular evolution using CODEML in PAML (Yang, 2007). Specifically, we tested branch, sites and branch (clade)–sites models. We compared branch models to a null M0 model with a single ω value, the M2a sites model (positive selection) to the null M1a (nearly neutral; Wong *et al.*, 2004), the branch–sites model A to the null (fixed_omega = 1, omega = 1), and the clade C model to M2a_rel. For branch, branch–sites and clade models, we labelled the two *PPC1* Agavoideae lineages and estimated ω separately; for *PPC2*, we labelled the single Agavoideae stem branch. Due to low phylogenetic resolution within the Agavoideae, specific tests for independent CAM origins within the subfamily were not feasible. FASTA files of multispecies alignments and NEWICK gene trees are available at www.github.com/kheyduk/AgavoideaeCAM.

Results

CAM in the Agavoideae

Gas exchange and leaf titratable acidity amounts implicated CAM in both *Hesperaloe* species and C₃ photosynthesis in *Hosta venusta* (Fig. 2; Tables S2, S3). Although we did not sample *Hosta venusta* under drought-stressed conditions, its thin leaf

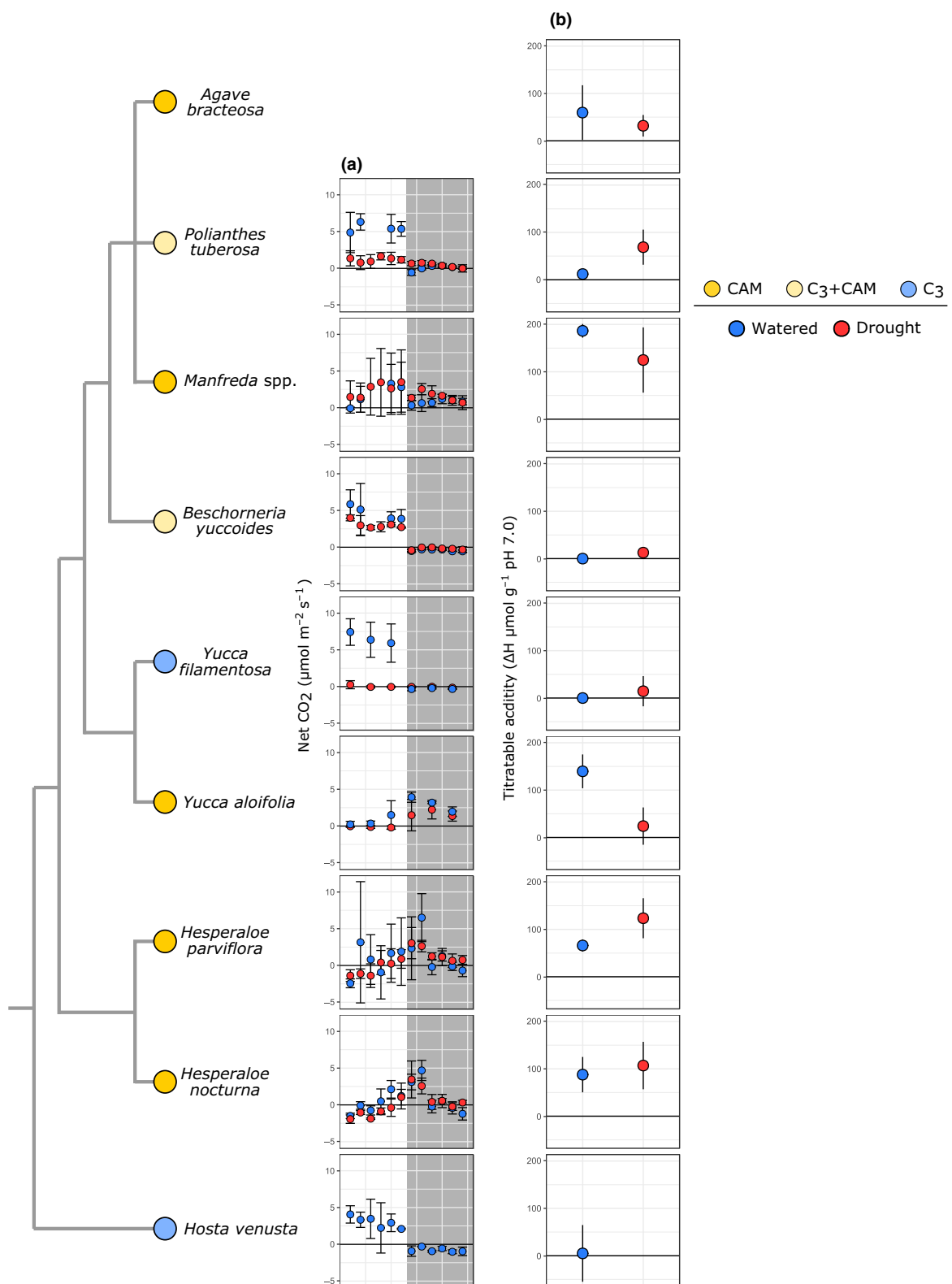


Fig. 2 Photosynthetic physiology of species in the Agavoideae. Species relationships are represented by the cladogram to the left; A (net photosynthesis, or the net flux of CO_2 per second per area), with shaded areas representing night time points (a); and the daily change in titratable leaf acidity ($\Delta\text{H } \mu\text{mol g}^{-1}$ in the early morning – late afternoon) (b); are shown per species, with means and standard errors calculated from replicates of each species. Colours next to species names indicate Crassulacean acid metabolism (CAM) (bright yellow), $\text{C}_3 + \text{CAM}$ (pale yellow), and C_3 (blue). Data for all species except *Hesperaloe* and *Hosta* comes from previous work (Heyduk *et al.*, 2018b, 2019b).

morphology (Heyduk *et al.*, 2016b) and shady, mesic habitat suggests it is very unlikely to use any mode of CAM photosynthesis. Most of the CAM species in the Agavoideae examined still rely at least partially on daytime CO₂ fixation by Rubisco (Fig. 2). Furthermore, *Yucca*, *Agave* and *Manfreda* all appear to downregulate CAM under drought stress, as seen in both their gas exchange patterns and titratable acidity levels under drought relative to well watered status (Fig. 2). *Hesperaloe parviflora* had slightly higher CO₂ uptake at night than did *H. nocturna*, although both had appreciable levels of acid accumulation and, unlike *Yucca* and *Agave* *sensu lato* species, had a slight upregulation of CAM under drought stress. Finally, as previously described (Heyduk *et al.*, 2018b), *Polianthes tuberosa* and *Beschorneria yuccoides* are C₃ + CAM, and both are able to facultatively use CAM under drought stress.

Cross-Agavoideae comparisons

The number of transcripts that showed significant time-structured expression varied across species, with the fewest in the C₃ species *Hosta venusta* ($n = 5576$) and the highest in the CAM species *Agave bracteosa* ($n = 28\,856$). Although *Hosta* was only assessed under well watered conditions, drought conditions are unlikely to have increased the total number of time-structured transcripts: across species, the transcripts that were both time structured and differentially expressed under drought represent a small proportion of the total time-structured transcripts (with the notable exception of *Agave*; Fig. 3a). All species that used C₃ photosynthesis or exhibit weak CAM had fewer transcripts that had a significant change in diurnal expression, with the exception of *Polianthes tuberosa*, which uses CAM facultatively more so than does *Beschorneria yuccoides* (Fig. 2). Many gene families (923) were time structured in all eight species (Table S4); 731 additional gene families were time structured in all species with the exception of *Hosta* (Fig. 3b; Table S5). This latter set included some canonical CAM genes, including both *PPC1* and *PPC2*, as well as phosphoenolpyruvate carboxylase kinase (*PPCK*), a kinase dedicated to the phosphorylation of PPC and thought to be required for efficient CAM (Taybi *et al.*, 2000), auxin-related response genes, and some genes related to light reactions (e.g. photosystem II reaction centre protein D).

The number of genes responsive to drought stress was far lower than the total number with time-structured expression, and the majority of drought-responsive genes had time-structured expression in at least one condition (watered or drought) (Fig. 3a,c). *Agave* had the largest number of differentially expressed genes under drought (*c.* 20%, Fig. 3a), while *H. nocturna* had the fewest (*c.* 2%). In both *Yucca* species, all drought-responsive genes were time structured in their expression. Examination of shared gene families of drought-responsive genes across the species showed that many gene families were unique to a particular species (Fig. 3c), suggesting that the drought response in the Agavoideae is variable and lineage specific.

Of the gene families with circadian clock annotations, over half (33/58) had significant time-structured expression in all eight species (Fig. 3d). Comparisons of phase (timing of peak

expression) across the eight species resulted in few differences in phase between species. In a comparison of CAM species (excluding *Agave* and *Beschorneria* due to low replicates/resolution; please refer to methods) vs C₃ species, only four gene families had a significant shift in phase: *Pseudo-response regulator 9* (*PPR9*), *Alfin-like* (*AFL*), *telomere binding protein* (*TRFL*), and a gene of unknown function (no *Arabidopsis* homologue, and BLAST hits are uncharacterised proteins) (Table S6). The comparison of phase changes between *Hosta* and the remainder of the Agavoideae species produced only a single gene family that had a shift in average timing of expression: *TRFL*, the same gene family found to be different between CAM and C₃ species. In general, expression patterns across species were highly similar; of the 265 gene families that were (1) common in all eight species and (2) significant cyclers as assessed by METACYCLE, only 17 had a shift in phase when testing for species as an explanatory factor ($P < 0.01$) (Table S7). To understand the evolution of phase, the mean phase per species of each of these 17 gene families was calculated, and from it we subtracted the mean phase of the gene family in *Hosta* (Fig. 3e). In the majority of these 17 gene families, the mean phase shift was low or was an instance in which one species had a large phase shift different from the remaining species (Fig. 3e), but none had a concerted C₃-to-CAM shift. In general, timing of expression was similar across all eight species in the majority of gene families.

PPC expression

Gene tree reconstruction of sequences placed in *PPC1* and *PPC2* gene families by ORTHOFINDER was largely consistent with previous analyses (Fig. 4) (Deng *et al.*, 2016; Heyduk *et al.*, 2019a). The *PPC1* tree shows a duplication event within monocot evolutionary history, after the divergence of the Dioscoreales (represented by *Dioscorea alata*) from the lineage leading to the last common ancestor of Asparagales and Poales (although *D. alata* appears to have a lineage-specific duplication). The monocot duplication event is independent from a similar duplication event in ancestral eudicots (Christin *et al.*, 2014; Silvera *et al.*, 2014). The placement of the *Acorus americanus* gene in the *PPC2* phylogeny as sister to all other sampled angiosperm homologues except *Amborella* is likely to be a result of the lack of other eudicots taxa in the analyses, or possibly eudicot-like mutations in the *A. americanus* *PPC2* gene. Regardless, the remainder of the gene tree is concordant with species relationships.

Although both major clades of *PPC1* were expressed in the Agavoideae, the overall expression levels of *PPC1-B* transcripts were much higher than for *PPC1-A*, particularly in CAM species (Fig. 5). *PPC1-B* expression also increased under drought notably in *Polianthes tuberosa*, a species known to engage in facultative CAM upon drought stress (Fig. 2). *PPC2* transcripts were highly expressed in both *Yucca aloifolia* and *Beschorneria yuccoides*, strong CAM and facultative-CAM species, respectively (Fig. 6). Expression of *PPC2* increased with drought in *Beschorneria*, consistent with increased CAM activity under drought conditions (Fig. 2). Three gene copies of *PPC2* were identified in the *Yucca aloifolia* genome, and all three had characteristic CAM-like

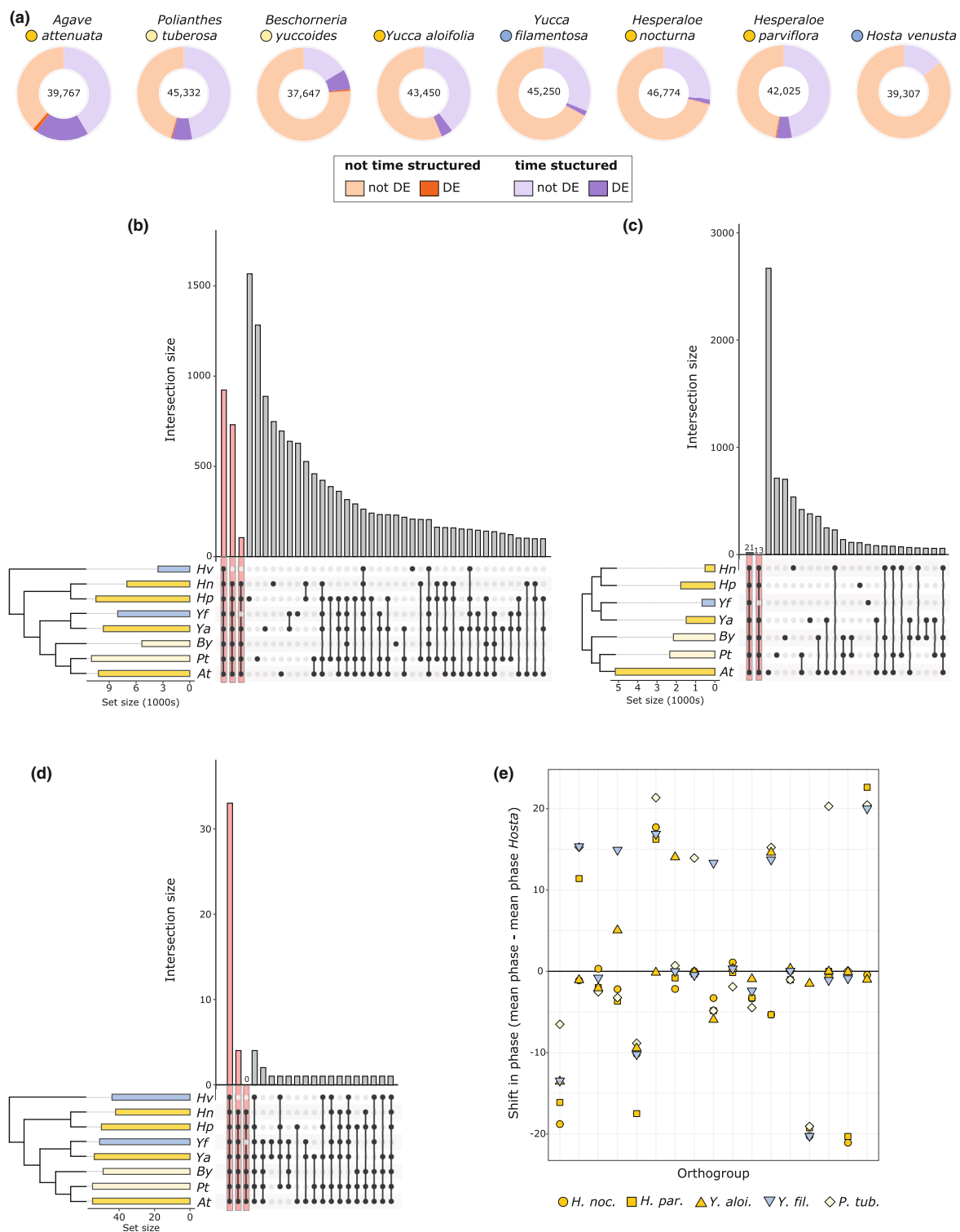


Fig. 3 (a) Total number of transcripts assessed in each species (centre), with a proportion of the transcripts showing significant time-structured expression (purple shades). A subset of both time-structured and not time-structured transcripts (orange shades) were differentially expressed (DE) under drought conditions (darker shades). (b) UpSet plot showing overlap in gene families (orthogroups from ORTHOFINDER) that were time structured across the eight species; bars on left of the species names indicate total number of gene families per species, colours indicate Crassulacean acid metabolism (CAM) (bright yellow), C₃ + CAM (pale yellow), and C₃ (blue). The same colour scheme is used for panels (b–e). The first three bars highlighted in pink indicate orthogroups shared across all species, across all species except *Hosta*, and across all CAM species. (c) Comparison of gene families that had differential expression under drought stress across seven of the eight species (*Hosta venusta* was not droughted). (d) Comparison of gene families with core circadian clock annotations that had time-structured expression across all eight species. (e) Shift in mean phase relative to *H. venusta* (mean phase of species – mean phase in *H. venusta*) in 17 gene families that had significantly different ($P < 0.01$) cycling across species as indicated by METACYCLE.

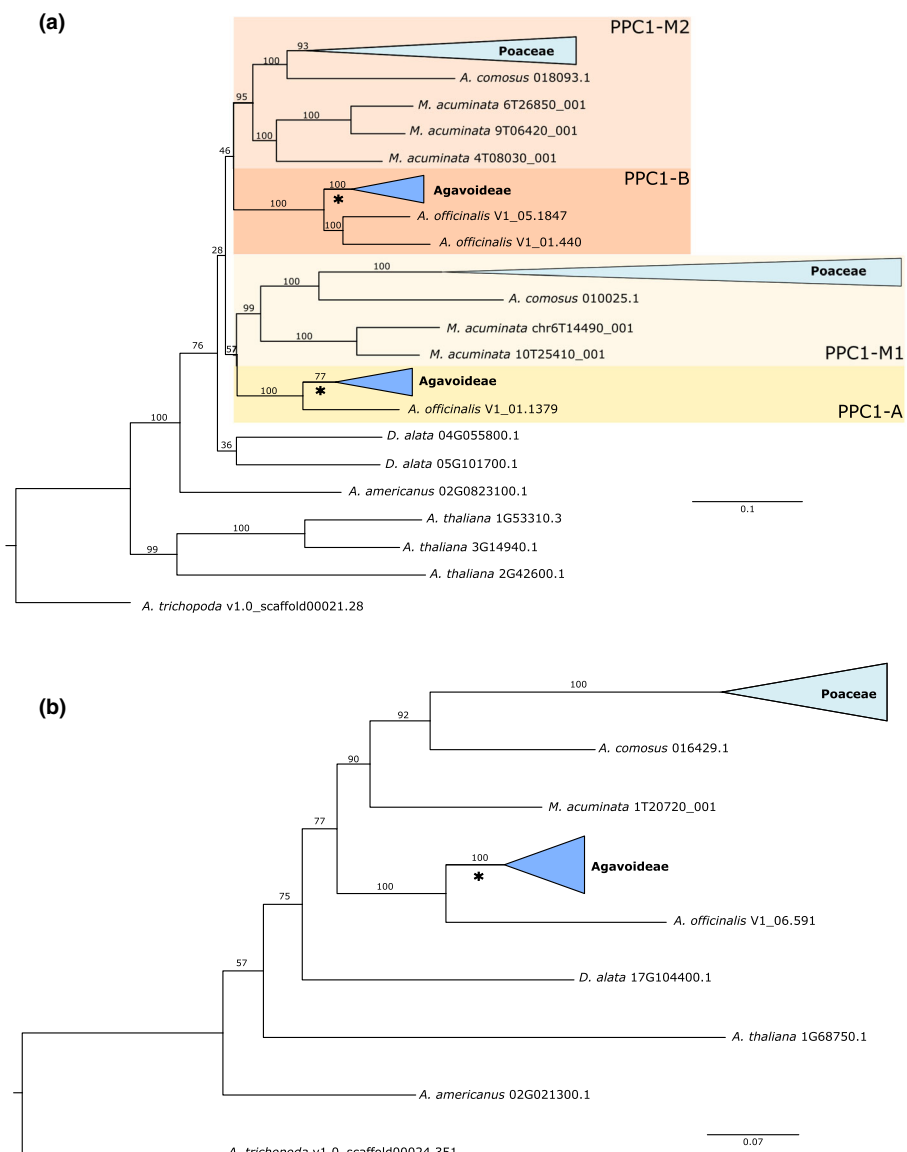


Fig. 4 Gene trees estimated with IQTREE for PPC1 (a) and PPC2 (b). Members of Poaceae and Agavoideae are collapsed for readability. All rapid bootstrap values are reported. Branches used for branch, branch \times sites and clade model tests in CODEML are subtended by an asterisk.

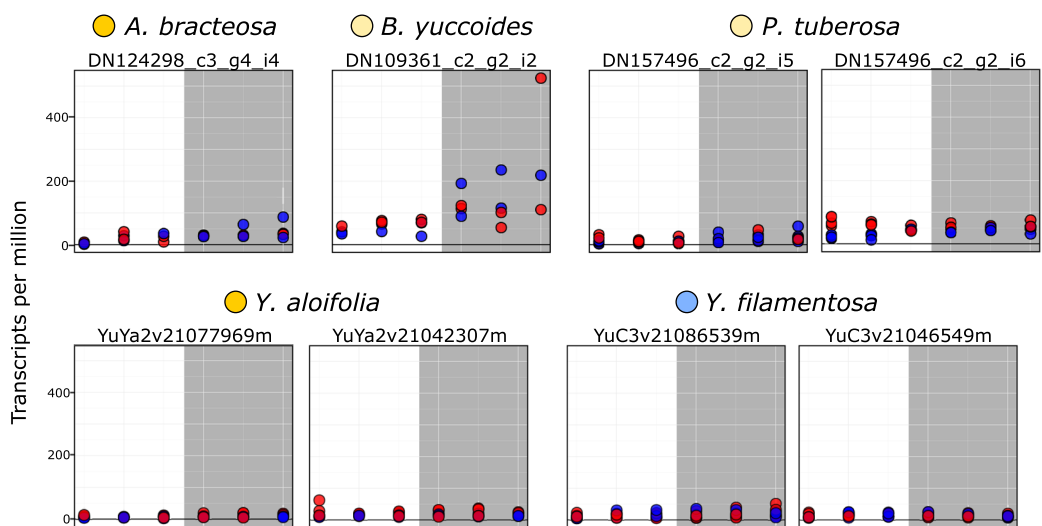
expression, with a peak before the onset of the dark period. Notably, *PPC2* is also expressed in a CAM-like pattern, albeit at lower levels, in the C₃ *Yucca filamentosa* (Fig. 6). This finding is consistent with previous RNA-seq analyses of *Yucca* (Heyduk *et al.*, 2019b). *Hesperaloe nocturna* gene expression is not shown in Fig. 5 because the lengths of PPC transcripts were too short, and therefore were filtered out from our gene tree estimation and subsequent expression analyses.

Molecular evolution of PPC genes

Assessment of changes in the strength and mode of selection assessed by the branch model revealed a significant shift in ω for *PPC1-A*, but not *PPC1-B* or *PPC2*. *PPC1-A* had a reduced ω relative to the background rate, suggesting increased purifying selection consistent with this gene's role in housekeeping pathways (Fig. 4; Tables 1, 2). The sites model tests for positive selection

were not significant for either *PPC1* or *PPC2* in the Agavoideae. However, *PPC1-B* had significant positive selection on some sites in the Agavoideae genes (Table 1), and Bayesian Empirical Bayes analysis revealed only one site under positive selection with a posterior probability >95%: a transition from an alanine to an asparagine at position 591. *PPC1-B* also exhibited shifts on constraint in the clade-sites test, with the Agavoideae having a third class of sites with weaker purifying selection compared with the background rate (0.44 on the foreground, 0.21 on the background, proportion of sites = 0.27). *PPC2* similarly only had a significant rejection of the sites null model in favour of the alternative clade model, with a third class of sites that had an elevated ω relative to background (0.52 on foreground, 0.18 on background, proportion of sites = 0.36) (Table 2). Together these results suggest that specific amino acid residues in Agavoideae *PPC1-B* and *PPC2* genes may be evolving under relaxed or positive selection.

(a) PPC1-A



(b) PPC1-B

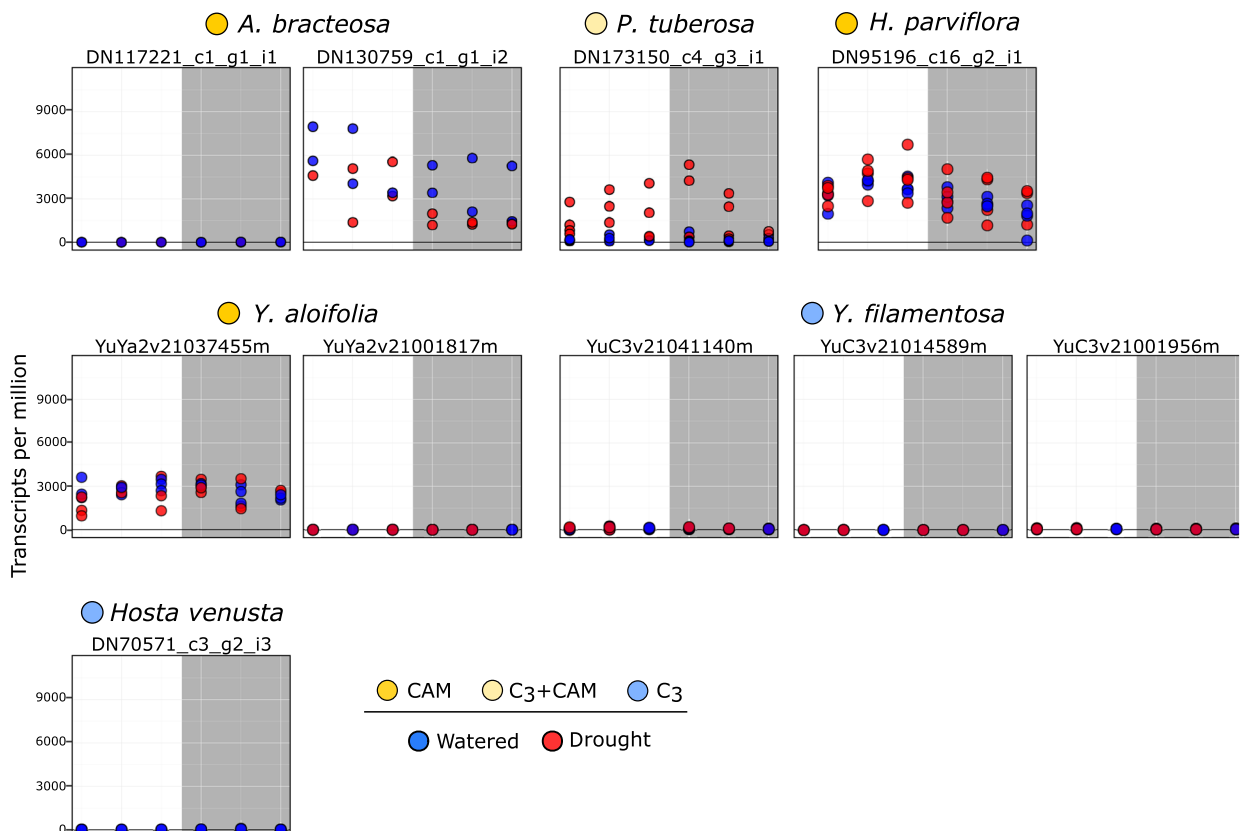


Fig. 5 Expression (transcripts per million) of PPC1 transcripts from the core Agavoideae species, shown separately for the two clades (a) and (b). Dots represent individual samples, with blue, well watered and red, drought stressed. Colours next to species names indicate Crassulacean acid metabolism (CAM) (bright yellow), C₃ + CAM (pale yellow), and C₃ (blue). Grey boxes indicates night time points. Transcripts are only shown here if they passed length and percentage identity filtering. *Hosta venusta* did not have drought-stressed samples taken for RNA sequencing.

PPC2

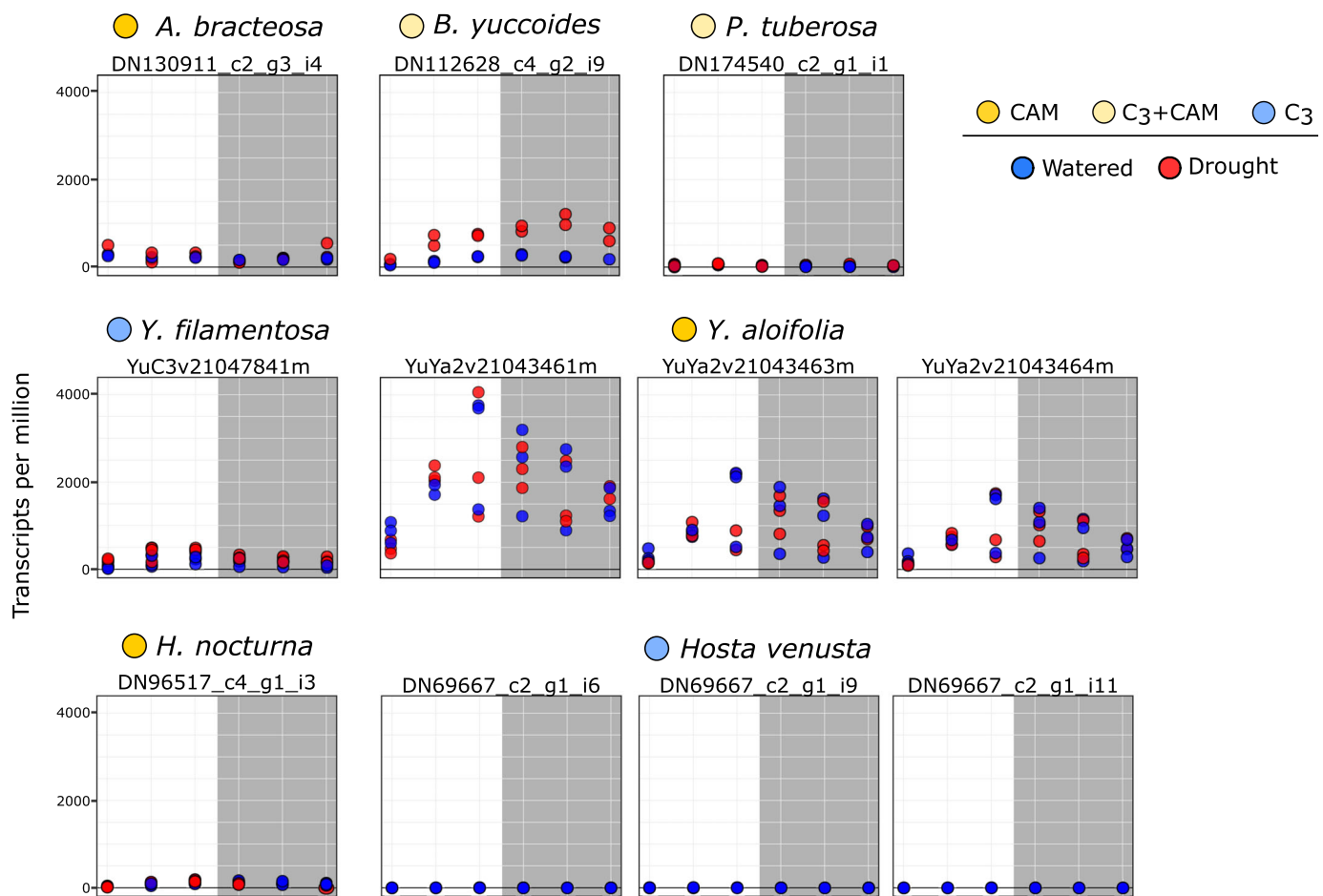


Fig. 6 Expression (transcripts per million) of PPC2 transcripts from the core Agavoideae species. Dots represent individual samples, with blue, well watered and red, drought stressed. Colours next to species names indicate Crassulacean acid metabolism (CAM; bright yellow), $C_3 + CAM$ (pale yellow), and C_3 (blue). Grey boxes indicates night time points. Transcripts are only shown here if they passed length and percentage identity filtering.

Discussion

Evolution of CAM in the Agavoideae

Previous work estimated three independent origins of CAM in the Agavoideae: one in the genus *Hesperaloe*, one in the genus *Yucca*, and one in *Agave* s.l. (Heyduk *et al.*, 2016b). However, this initial estimation was based on carbon isotope values, which cannot separate $C_3 + CAM$ from C_3 in the majority of cases (Winter *et al.*, 2015). Detailed physiological measurements under both well watered and drought-stressed conditions revealed that *Polianthes* had the ability to upregulate CAM under drought stress, although maintains low-level CAM even under well watered conditions. *Beschorneria* has a very slight CAM increase at night, indicated by a small shift in titratable acidities and a decrease in nighttime respiration (Heyduk *et al.*, 2018b). *Yucca* species are divided, in that nearly half are expected to use C_3 and the other half are likely to be CAM; these inferences are based on carbon isotopes, and warrant more detailed physiological assessment beyond the two species included in this study and a handful

of others (Smith *et al.*, 1983; Heyduk *et al.*, 2016a). The presence of CAM was confirmed in *Hesperaloe*, with both species in this study exhibiting strong CAM (Fig. 2). *Hosta* showed no evidence of CAM in our study, although it was not drought stressed. Based on gene expression patterns detected here, as well as anatomical traits and carbon isotope values (Heyduk *et al.*, 2016b), we do not expect *Hosta* to be able to upregulate CAM under drought stress. Together these separate physiological assessments across the Agavoideae confirmed the presence of CAM in *Hesperaloe*, *Yucca* and *Agave* s.l. and furthered our understanding of intermediate CAM species (e.g. *Polianthes* and *Beschorneria*).

Conservation and novelty in gene expression

Across diverse plant species, roughly 20–60% of transcripts show some time-of-day differential expression (Covington *et al.*, 2008; Hayes *et al.*, 2010; Filichkin *et al.*, 2011; Lai *et al.*, 2020), however *Arabidopsis* has up to 89% of transcripts cycling under at least one experimental time course condition (Michael *et al.*, 2008). In *Sedum album*, which has the ability to

Table 1 Results from tests of selection on PPC1.

Branch	Model	ω^1	InL	np ²	Significance ³
na	M0	$\omega = 0.077$	-52767.838	110	na
PPC1-A	Branch	$\omega_b = 0.078, \omega_f = 0.013$	-52762.554	111	LR = 10.57, P = 0.001
PPC1-B	Branch	$\omega_b = 0.077, \omega_f = 0.065$	-52767.705	111	LR = 0.265, P = 0.608
na	Sites, M1a (nearly neutral)	$\omega_1 = 0.059 (p_1 = 0.92), \omega_2 = 1 (p_2 = 0.08)$	-52185.176	111	na
na	Sites, M2a (positive selection)	$\omega_1 = 0.059 (p_1 = 0.92), \omega_2 = 1 (p_2 = 0.05), \omega_3 = 1 (p_3 = 0.03)$	-52185.176	113	LR = 0
PPC1-A	MA null	0[$\omega_b = 0.059, \omega_f = 0.059, p = 0.92$], 1[$\omega_b = 1, \omega_f = 1, p = 0.08$], 2a[$\omega_b = 0.059, \omega_f = 1, p = 0$], 2b[$\omega_b = 1, \omega_f = 1, p = 0$]	-52185.176	112	na
PPC1-A	MA	0[$\omega_b = 0.059, \omega_f = 0.059, p = 0.92$], 1[$\omega_b = 1, \omega_f = 1, p = 0.08$], 2a[$\omega_b = 0.059, \omega_f = 39.8, p = 0.002$], 2b[$\omega_b = 1, \omega_f = 1, p = 0$]	-52185.176	113	LR = 0
PPC1-B	MA null	0[$\omega_b = 0.059, \omega_f = 0.059, p = 0.92$], 1[$\omega_b = 1, \omega_f = 1, p = 0.08$], 2a[$\omega_b = 0.059, \omega_f = 1, p = 0$], 2b[$\omega_b = 1, \omega_f = 1, p = 0$]	-52185.176	112	na
PPC1-B	MA	0[$\omega_b = 0.059, \omega_f = 0.059, p = 0.92$], 1[$\omega_b = 1, \omega_f = 1, p = 0.08$], 2a[$\omega_b = 0.059, \omega_f = 39.8, p = 0.002$], 2b[$\omega_b = 1, \omega_f = 1, p = 0.0002$]	-52182.449	113	LR = 5.45, P = 0.019
na	M2a_rel (null for clade-sites C tests)	$\omega_1 = 0.02 (p_1 = 0.72), \omega_2 = 1 (p_2 = 0.02), \omega_3 = 0.22 (p_3 = 0.26)$	-51414.294	113	na
PPC1-A	Clade-sites C	0[$\omega_b = 0.02, \omega_f = 0.02, p = 0.72$], 1[$\omega_b = 1, \omega_f = 1, p = 0.016$], 2[$\omega_b = 0.23, \omega_f = 0.27, p = 0.26$]	-51413.361	114	LR = 1.87, P = 0.17
PPC1-B	Clade-sites C	0[$\omega_b = 0.02, \omega_f = 0.02, p = 0.71$], 1[$\omega_b = 1, \omega_f = 1, p = 0.02$], 2[$\omega_b = 0.21, \omega_f = 0.44, p = 0.27$]	-51392.506	114	LR = 43.58, P < 0.001

¹Values reported for background, foreground, in which foreground is the branch of interest in the Agavoideae; for sites models, three classes of omegas and proportion of sites (p) in each class are reported; for branch \times sites models, foreground and background values for omega are reported plus a proportion of sites in each site class (0, 1, 2a and 2b).

²Number of parameters.

³Based on a likelihood ratio test which is χ^2 distributed. na, null models that were not tested against any other null.

facultatively upregulate CAM, there is a slight increase in the number of cycling transcripts when plants use CAM compared with C₃ (41% vs 35%, respectively) (Wai *et al.*, 2019). The number of time-structured transcripts in Agavoideae species varied, with *Hosta* having the fewest transcripts that were time structured, and *Agave* having the greatest number. The number of time-structured transcripts did not correlate with the presence of CAM; for example, *Y. filamentosa* and *Y. aloifolia* had similar numbers of time-structured transcripts, despite differences in photosynthetic pathway. Similarly, *Agave* and *Polianthes* both had many transcripts with diel variation, despite *Polianthes* being only weakly, facultatively CAM (Fig. 3). *Beschorneria*, which is sister to *Polianthes* and *Agave*, showed the smallest number of time-structured transcripts, although it is also the weakest CAM species measured across these species.

Very few gene families had time-structured expression across all CAM species ($n = 105$ in all CAM, $n = 126$ in strong CAM). Two key genes related to CAM – *PPC2* (although, notably, not *PPC1*) and *PPCK* – were time structured in all species except *Hosta* (i.e. including the C₃ *Y. filamentosa*). *PPCK* in particular has been shown to have direct and reciprocal clock connections; knockdowns of

PPCK in *Kalanchoë fedtschenkoi* had significantly reduced CAM and the lack of circadian oscillation in *PPCK* perturbed oscillation patterns of core clock genes (Boxall *et al.*, 2017). Knockdown of *PPC1* in *Kalanchoë laxiflora* also resulted in changes to the oscillation patterns and amplitude of clock genes, although notably a different set of core clock genes was affected by *PPC1* knockdowns relative to *PPCK* (Boxall *et al.*, 2020). The integration of the circadian clock and CAM pathway genes is clearly important for CAM physiology, although the presence and cycling of these genes does not, alone, lead to CAM ability; *Y. filamentosa* has cycling of these gene families (e.g. *PPC2*), but expression levels are either too low or transcripts are affected by other post-translational modifications to render them insufficient for CAM (Heyduk *et al.*, 2019b). Moreover, we found a lack of shared gene families with shifts to time-structured expression across CAM species in the Agavoideae, which suggests three hypotheses: (1) the repeated evolution of CAM has involved lineage-specific changes to the molecular networks rather than parallelisms, (2) gene re-wiring happened in the ancestor of the Agavoideae and facilitated the repeated evolution of CAM, or (3) the overall scope of re-wiring of gene expression into the clock is limited for CAM.

Table 2 Results from tests of selection on PPC2.

Model	ω^1	lnL	np ²	Significance ³
M0	$\omega = 0.126$	-27536.821	44	na
Branch	$\omega_b = 0.126, \omega_f = 0.115$	-27536.753	45	LR = 0.136, P = 0.71
Sites, M1a (nearly neutral)	$\omega_1 = 0.07 (p_1 = 0.82), \omega_2 = 1 (p_2 = 0.18)$	-26777.829	45	na
sites, M2a (positive selection)	$\omega_1 = 0.07 (p_1 = 0.82), \omega_2 = 1 (p_2 = 0.09), \omega_3 = 1 (p_3 = 0.09)$	-26777.829	47	LR = 0
MA null	0[$\omega_b = 0.065, \omega_f = 0.065, p = 0.82$], 1[$\omega_b = 1, \omega_f = 1, p = 0.18$], 2a[$\omega_b = 0.07, \omega_f = 1, p = 0$], 2b[$\omega_b = 1, \omega_f = 1, p = 0$]	-26777.829	46	na
MA	0[$\omega_b = 0.065, \omega_f = 0.065, p = 0.82$], 1[$\omega_b = 1, \omega_f = 1, p = 0.18$], 2a[$\omega_b = 0.07, \omega_f = 1, p = 0$], 2b[$\omega_b = 1, \omega_f = 1, p = 0$]	-26777.829	47	LR = 0
M2a_rel (null for clade-sites C tests)	$\omega_1 = 0.02 (p_1 = 0.59), \omega_2 = 1 (p_2 = 0.09), \omega_3 = 0.23 (p_3 = 0.33)$	-26537.435	47	na
Clade-sites C	0[$\omega_b = 0.01, \omega_f = 0.01, p = 0.55$], 1[$\omega_b = 1, \omega_f = 1, p = 0.09$], 2[$\omega_b = 0.18, \omega_f = 0.52, p = 0.36$]	-26508.092	48	LR = 58.68, P < 0.001

¹Values reported for background, foreground, in which foreground is the branch of interest in the Agavoideae; for sites models, three classes of omegas and proportion of sites in each class are reported; for branch \times sites models, foreground and background values for omega are reported plus proportion of sites in each site class (0, 1, 2a and 2b).

²Number of parameters.

³Based on a likelihood ratio test that is χ^2 distributed. na, null models that were not tested against any other null.

Assessing the 24-h time-structured variation of gene expression in CAM and C₃ lineages has confirmed the important role of clock integration with CAM metabolic genes, but generally has not revealed any master regulator of CAM. Most studies highlight the conservation of circadian clock components and the timing of their expression, regardless of the photosynthetic pathway (Moseley *et al.* 2018; Wai & VanBuren, 2018; Yin *et al.* 2018; Wai *et al.* 2019). Researchers have focused on the few aspects of the clock that are different between C₃ and CAM comparisons. For example, *PRR9* in *Opuntia* (CAM) was shown to have a change in phase compared with the *Arabidopsis* orthologue (Mallona *et al.* 2011), comparisons between *Kalanchoe* and *Arabidopsis* showed phase shifts in some evening elements, including *ELF3/4* and *LUX* (Moseley *et al.* 2018), and *Agave* had shifted expression of RVE, a clock output gene, relative to *Arabidopsis* (Yin *et al.* 2018). In the Agavoideae, the majority of circadian gene families had shared phase of expression across all eight species. Of those gene families that had a significant species effect in the phase of expression, few had extreme phase shifts or showed consistent C₃ vs CAM differences. Our findings, together with those of other studies assessing core circadian regulators in CAM lineages, pointed to an overall conservation of the circadian clock, even in plants with a strong CAM physiology (Boxall *et al.* 2020). However, it is worth noting that the majority of comparative transcriptomics studies in CAM, including this one, assessed temporal variation in expression over a single day : night period, making it difficult to pinpoint which genes were responsible for clock inputs into the CAM pathway, and which were downstream targets. Many studies still rely on distant outgroups for comparison (typically *Arabidopsis*), and therefore continue to confound changes associated with CAM to those that have arisen simply due to evolutionary divergence. Future work on the nature of gene expression and evolution in CAM species should

endeavour to use free-running conditions to better assess the roles of the circadian clock in CAM species, and should carefully select comparison species to minimise evolutionary distance. Regardless, it seems unlikely that large perturbations to the circadian clock are required for the evolution of CAM from a C₃ ancestor; instead, changes to promoter sequences and regulatory regions of genes contributing to CAM may have a larger role to play in altering the timing and magnitude of their expression.

Unlike the relatively conserved number and type of genes that exhibited time-structured variation in gene expression, the response to drought was highly lineage specific. A large proportion of gene families was uniquely differentially expressed in a singular species. Although the present study includes comparisons across three separate experiments (Heyduk *et al.* 2018b, 2019b), even species drought stressed in the same experiment showed vastly different responses to drought. While plant water status was monitored in all experiments by the proxy of soil moisture content (Table S1), even the same soil moisture content can variably affect plants of different ages, genotypes and species. *Agave*'s strong differential regulation to drought is surprising given its constitutive CAM physiology that is thought to buffer against the effects of drought stress. Indeed, the majority of CAM species studied here was affected by drought: *Y. aloifolia*, *A. bracteosa*, and *Manfreda* sp. all exhibited decreases in titratable leaf acidity and, in *Yucca* and *Manfreda*, drops in nocturnal CO₂ assimilation. The effects of drought stress on CAM physiology are vastly understudied, although work has been done in facultative-CAM species (Cushman *et al.* 2008; Wai *et al.* 2019; Heyduk *et al.* 2021). Both the physiological and gene expression data presented here suggested that full CAM species are not immune to the effects of drought, and indeed exhibit strong physiological and transcriptional responses. Finally, for all species studied here, the majority of drought-responsive genes were also

time structured; in other words, constitutively expressed genes were infrequently affected by drought stress.

Gene recruitment for CAM photosynthesis

In almost all published instances of C₄ or CAM evolution (please refer to Wickell *et al.*, 2021 for a notable exception), the PPC gene copy that was recruited was from a gene family known as the 'plant' PPCs, or PPC1. PPC1 is used by all plants for the replenishment of intermediates in the TCA cycle, and a singular copy typically gets re-wired for C₄ or CAM (Heyduk *et al.*, 2019a). The clear CAM-like expression of PPC2 in *Yucca aloifolia* and, to a lesser extent, *Beschorneria yuccoides*, suggests that both of these species have recruited PPC2 as an alternate carboxylating enzyme for CAM. PPC1 is still expressed in both of these species, and supports previous work that suggests PPC2 that forms a hetero-octamer with PPC1 (O'Leary *et al.*, 2011), although this remains to be tested in the Agavoideae. Although we cannot say for certain PPC2 protein is produced, it seems unlikely that the transcripts would be expressed so highly (> 1000 TPM) in *Yucca aloifolia* with no functional consequence. Moreover, expression of PPC2 in *Yucca aloifolia* peaks right before the onset of the night period, consistent with expression patterns of PPCs in other Agavoideae in this study, as well as expression profiles of PPC in other lineages (Ming *et al.*, 2015; Abraham *et al.*, 2016; Yang *et al.*, 2017; Heyduk *et al.*, 2018a; Wai *et al.*, 2019). The overall carboxylase activity of PPC2 in the Agavoideae remains to be studied, but could lend further clues to how this atypical gene copy was recruited into the CAM pathway.

Unlike C₄ PPCs, in which convergent amino acid substitutions seem key to the recruitment of PPC1 gene copies into the C₄ pathway (Christin *et al.*, 2007; Rosnow *et al.*, 2014; Goolsby *et al.*, 2018), evidence for convergent evolution at the molecular level in CAM is lacking. A comparison of PPC sequences between *Kalanchoë* and *Phalaenopsis* did reveal a shared amino acid change from R/H/K to D and was shown to significantly increase the activity of PPC (Yang *et al.*, 2017). However, this amino acid substitution is not ubiquitous in CAM species; it is absent from *Ananas* (Yang *et al.*, 2017) and all members of the Agavoideae examined here (please refer to the github repository for FASTA files), suggesting that either the shared mutation is due to homoplasy, or may be convergent but not essential for CAM. Our results further suggest that overall PPC genes are conserved, even when they are being recruited into the CAM pathway (Tables 1 and 2). In general, the lability of CAM as a phenotype, as well as the wide diversity of lineages in which it evolves, seems to allow variable pathways to organise the genetic requirements, including which major copy of the main carboxylating enzyme, PPC, is recruited. Increasing the number of CAM lineages studied physiologically and genetically will allow us to determine whether novel mechanisms of evolving CAM – such as the recruitment of PPC2 in the Agavoideae – are indeed rare, or more common across green plants.

By comparing RNA-seq data across closely related species that span multiple origins of CAM, we have shown that most gene families have diurnal variation in gene expression, regardless of

photosynthetic status. In particular, core circadian clock genes are similarly expressed across all the species examined here. By contrast, drought response was highly lineage specific, and suggests that lineages have fine tuned or independently evolved their drought response gene networks. While historically CAM in the Agavoideae has been thought to be the result of three independent origins, we cannot rule out a single origin of CAM with subsequent reversals to C₃. However, reversals to C₃ from CAM appear to be rare in angiosperms, and the recruitment of PPC2 for CAM function in *Yucca* (and to a lesser extent in *Beschorneria*) supports the inference of independent origins of CAM in the Agavoideae and furthers the idea that the evolutionary routes to CAM are markedly variable.

Acknowledgements

The authors would like to acknowledge the UGA Plant Biology glasshouse staff for the help in maintaining plants, the Georgia Advanced Computing Resources Center and the University of Hawai'i Information Technology Services – Cyberinfrastructure for computational support, and Amanda L. Cummings and Richard Field for assistance with glasshouse and lab work. This work was supported by funding from NSF (DEB1442199 to JL-M) and a Yale Institute for Biospheric Studies Donnelley Fellowship (to KH). We thank the Department of Energy Joint Genome Institute and collaborators for access to pre-publication data for *Acorus americanus* v.1.1, *Yucca aloifolia* and *Yucca filamentosa*.

Author contributions

KH conducted physiology experiments, sampled for RNA, prepared sequencing libraries and analysed data; EVM conducted molecular evolution analyses; JL-M helped with framing and data interpretation; all three authors contributed to writing and editing the manuscript.

ORCID

Karolina Heyduk  <https://orcid.org/0000-0002-1429-6397>
Jim Leebens-Mack  <https://orcid.org/0000-0003-4811-2231>
Edward V. McAssey  <https://orcid.org/0000-0003-1568-3361>

Data availability

Raw sequencing data generated in this study are available on the NCBI SRA, under BioProject PRJNA755802. Processed RNA-seq counts and TPM files, as well as FASTA files for PPC1 and PPC2 molecular evolution analyses, are available at <https://github.com/kheyduk/AgavoideaeComparative>.

References

Abraham PE, Yin H, Borland AM, Weighill D, Lim SD, De Paoli HC, Engle N, Jones PC, Agh R, Weston DJ *et al.* 2016. Transcript, protein and metabolite temporal dynamics in the CAM plant *Agave*. *Nature Plants* 2: 16178.

Amborella Genome Project. 2013. The *Amborella* genome and the evolution of flowering plants. *Science* 342: 1241089.

Aubry S, Kelly S, Kumpers BMC, Smith-Unna RD, Hibberd JM. 2014. Deep evolutionary comparison of gene expression identifies parallel recruitment of trans-factors in two independent origins of C₄ photosynthesis. *PLoS Genetics* 10: e1004365.

Bennetzen JL, Schmutz J, Wang H, Percifield R, Hawkins J, Pontaroli AC, Estep M, Feng L, Vaughn JN, Grimwood J et al. 2012. Reference genome sequence of the model plant *Setaria*. *Nature Biotechnology* 30: 555–561.

Bolger AM, Lohse M, Usadel B. 2014. TRIMOMATIC: a flexible trimmer for Illumina sequence data. *Bioinformatics* 30: 2114–2120.

Boxall SF, Dever LV, Kneřová J, Gould PD, Hartwell J. 2017. Phosphorylation of phosphoenolpyruvate carboxylase is essential for maximal and sustained dark CO₂ fixation and core circadian clock operation in the obligate crassulacean acid metabolism species *Kalanchoe fedtschenkoi*. *Plant Cell* 29: 2519–2536.

Boxall SF, Kadu N, Dever LV, Kneřová J, Waller JL, Gould PJD, Hartwell J. 2020. *Kalanchoe* PPC1 is essential for Crassulacean acid metabolism and the regulation of core circadian clock and guard cell signaling genes. *Plant Cell* 32: 1136–1160.

Bräutigam A, Schliesky S, Külahoglu C, Osborne CP, Weber APM. 2014. Towards an integrative model of C₄ photosynthetic subtypes: insights from comparative transcriptome analysis of NAD-ME, NADP-ME, and PEP-CK C₄ species. *Journal of Experimental Botany* 65: 3579–3593.

Bray NL, Pimentel H, Melsted P, Pachter L. 2016. Near-optimal probabilistic RNA-seq quantification. *Nature Biotechnology* 34: 525–527.

Bredeson JV, Lyons JB, Oniyinde IO, Okereke NR, Kolade O, Nnabue I, Nwadihi CO, Hřibová E, Parker M, Nwogha J et al. 2022. Chromosome evolution and the genetic basis of agronomically important traits in greater yam. *Nature Communications* 13: 2001.

Brilhaus D, Bräutigam A, Mettler-Altmann T, Winter K, Weber APM. 2016. Reversible burst of transcriptional changes during induction of crassulacean acid metabolism in *Talinum triangulare*. *Plant Physiology* 170: 102–122.

Ceusters J, Borland AM, Taybi T, Frans M, Godts C, De Proft MP. 2014. Light quality modulates metabolic synchronization over the diel phases of Crassulacean acid metabolism. *Journal of Experimental Botany* 65: 3705–3714.

Cheng C-Y, Krishnakumar V, Chan AP, Thibaud-Nissen F, Schobel S, Town CD. 2017. Araport11: a complete reannotation of the *Arabidopsis thaliana* reference genome. *The Plant Journal* 89: 789–804.

Christin P-A, Arakaki M, Osborne CP, Bräutigam A, Sage RF, Hibberd JM, Kelly S, Covshoff S, Wong GK-S, Hancock L et al. 2014. Shared origins of a key enzyme during the evolution of C₄ and CAM metabolism. *Journal of Experimental Botany* 65: 3609–3621.

Christin P-A, Boxall SF, Gregory R, Edwards EJ, Hartwell J, Osborne CP. 2013. Parallel recruitment of multiple genes into C₄ photosynthesis. *Genome Biology and Evolution* 5: 2174–2187.

Christin P-A, Salamin N, Savolainen V, Duvall MR, Besnard G. 2007. C₄ photosynthesis evolved in grasses via parallel adaptive genetic changes. *Current Biology* 17: 1241–1247.

Christin P-A, Samaritani E, Petitpierre B, Salamin N, Besnard G. 2009. Evolutionary insights on C₄ photosynthetic subtypes in grasses from genomics and phylogenetics. *Genome Biology and Evolution* 1: 221–230.

Conesa A, Nueda MJ, Ferrer A, Talón M. 2006. MASiGPRO: a method to identify significantly differential expression profiles in time-course microarray experiments. *Bioinformatics* 22: 1096–1102.

Conway JR, Lex A, Gehlenborg N. 2017. UPSETR: an R package for the visualization of intersecting sets and their properties. *Bioinformatics* 33: 2938–2940.

Covington MF, Malof JN, Straume M, Kay SA, Harmer SL. 2008. Global transcriptome analysis reveals circadian regulation of key pathways in plant growth and development. *Genome Biology* 9: R130.

Cushman JC, Tillett RL, Wood JA, Branco JM, Schlauch KA. 2008. Large-scale mRNA expression profiling in the common ice plant, *Mesembryanthemum crystallinum*, performing C₃ photosynthesis and Crassulacean acid metabolism (CAM). *Journal of Experimental Botany* 59: 1875–1894.

D'Hont A, Denoeud F, Aury J-M, Baurens F-C, Carreel F, Garsmeur O, Noel B, Bocs S, Droc G, Rouard M et al. 2012. The banana (*Musa acuminata*) genome and the evolution of monocotyledonous plants. *Nature* 488: 213–217.

Deng H, Zhang L-S, Zhang G-Q, Zheng B-Q, Liu Z-J, Wang Y. 2016. Evolutionary history of PEPC genes in green plants: implications for the evolution of CAM in orchids. *Molecular Phylogenetics and Evolution* 94: 559–564.

Denoeud F, Carretero-Paulet L, Dereeper A, Droc G, Guyot R, Pietrella M, Zheng C, Alberti A, Anthony F, Aprea G et al. 2014. The coffee genome provides insight into the convergent evolution of caffeine biosynthesis. *Science* 345: 1181–1184.

Edwards EJ. 2019. Evolutionary trajectories, accessibility, and other metaphors: the case of C₄ and CAM photosynthesis. *The New Phytologist* 223: 1752–1755.

Emms DM, Kelly S. 2019. ORTHOFINDER: phylogenetic orthology inference for comparative genomics. *Genome Biology* 20: 238.

Eronen JT, Fortelius M, Micheels A, Portmann FT, Puolamäki K, Janis CM. 2012. Neogene aridification of the Northern Hemisphere. *Geology* 40: 823–826.

Filichkin SA, Breton G, Priest HD, Dharmawardhana P, Jaiswal P, Fox SE, Michael TP, Chory J, Kay SA, Mockler TC. 2011. Global profiling of rice and poplar transcriptomes highlights key conserved circadian-controlled pathways and cis-regulatory modules. *PLoS ONE* 6: e16907.

Gennidakis S, Rao S, Greenham K, Uhrig RG. 2007. Bacterial- and plant-type phosphoenolpyruvate carboxylase polypeptides interact in the hetero-oligomeric class-2 PEPC complex of developing castor oil seeds. *The Plant Journal* 52: 839–849.

Glenn TC, Nilsen RA, Kieran TJ, Sanders JG, Bayona-Vásquez NJ, Finger JW, Pierson TW, Bentley KE, Hoffberg SL, Louha S et al. 2019. Adapterama I: universal stubs and primers for 384 unique dual-indexed or 147,456 combinatorially-indexed Illumina libraries (iTru & iNext). *PeerJ* 7: e7755.

Glynn EF, Chen J, Mushegian AR. 2005. Detecting periodic patterns in unevenly spaced gene expression time series using Lomb–Scargle periodograms. *Bioinformatics* 22: 310–316.

Goodstein DM, Shu SQ, Howson R, Neupane R, Hayes RD, Fazo J. 2012. PHYTOZOME: a comparative platform for green plant genomics. *Nucleic Acids Research* 40: D1178–D1186.

Goolsby EW, Moore AJ, Hancock LP, De Vos JM, Edwards EJ. 2018. Molecular evolution of key metabolic genes during transitions to C₄ and CAM photosynthesis. *American Journal of Botany* 105: 602–613.

Grabherr MG, Haas BJ, Yassour M, Levin JZ, Thompson DA, Amit I, Adiconis X, Fan L, Raychowdhury R, Zeng Q et al. 2011. Full-length transcriptome assembly from RNA-Seq data without a reference genome. *Nature Biotechnology* 29: 644–652.

Harkess A, Zhou J, Xu C, Bowers JE, Van der Hulst R, Ayyampalayam S, Mercati F, Riccardi P, McKain MR, Kakrana A et al. 2017. The asparagus genome sheds light on the origin and evolution of a young Y chromosome. *Nature Communications* 8: 1279.

Hayes KR, Beatty M, Meng X, Simmons CR, Habben JE, Danilevskaya ON. 2010. Maize global transcriptomics reveals pervasive leaf diurnal rhythms but rhythms in developing ears are largely limited to the core oscillator. *PLoS ONE* 5: e12887.

Heyduk K, Burrell N, Lalani F, Leebens-Mack J. 2016a. Gas exchange and leaf anatomy of a C₃-CAM hybrid, *Yucca gloriosa* (Asparagaceae). *Journal of Experimental Botany* 67: 1369–1379.

Heyduk K, Hwang M, Albert V, Silvera K, Lan T, Farr K, Chang T-H, Chan M-T, Winter K, Leebens-Mack J. 2018a. Altered gene regulatory networks are associated with the transition from C₃ to Crassulacean acid metabolism in *Erycina* (Oncidiinae: Orchidaceae). *Frontiers in Plant Science* 9: 2000.

Heyduk K, McKain MR, Lalani F, Leebens-Mack J. 2016b. Evolution of CAM anatomy predates the origins of Crassulacean acid metabolism in the Agavoideae (Asparagaceae). *Molecular Phylogenetics and Evolution* 105: 102–113.

Heyduk K, Moreno-Villena JJ, Gilman IS, Christin P-A, Edwards EJ. 2019a. The genetics of convergent evolution: insights from plant photosynthesis. *Nature Reviews Genetics* 20: 485–493.

Heyduk K, Ray JN, Ayyampalayam S, Leebens-Mack J. 2018b. Shifts in gene expression profiles are associated with weak and strong Crassulacean acid metabolism. *American Journal of Botany* 105: 587–601.

Heyduk K, Ray JN, Ayyampalayam S, Moledina N, Borland A, Harding SA, Tsai C-J, Leebens-Mack J. 2019b. Shared expression of Crassulacean acid

metabolism (CAM) genes predates the origin of CAM in the genus *Yucca*. *Journal of Experimental Botany* 70: 6597–6609.

Heyduk K, Ray JN, Leebens-Mack J. 2021. Leaf anatomy is not correlated to CAM function in a C₃+CAM hybrid species, *Yucca gloriosa*. *Annals of Botany* 4: 437–449.

Hughes ME, Hogenesch JB, Kornacker K. 2010. JTK CYCLE: an efficient nonparametric algorithm for detecting rhythmic components in genome-scale data sets. *Journal of Biological Rhythms* 25: 372–380.

Igawa T, Fujiwara M, Tanaka I, Fukao Y, Yanagawa Y. 2010. Characterization of bacterial-type phosphoenolpyruvate carboxylase expressed in male gametophyte of higher plants. *BMC Plant Biology* 10: 200.

International Brachypodium Initiative. 2010. Genome sequencing and analysis of the model grass *Brachypodium distachyon*. *Nature* 463: 763–768.

Lai X, Bendix C, Yan L, Zhang Y, Schnable JC, Harmon FG. 2020. Interspecific analysis of diurnal gene regulation in panicoide grasses identifies known and novel regulatory motifs. *BMC Genomics* 21: 428.

Langmead B, Salzberg SL. 2012. Fast gapped-read alignment with Bowtie 2. *Nature Methods* 9: 357–359.

Mallona I, Egea-Cortines M, Weiss J. 2011. Conserved and divergent rhythms of Crassulacean acid metabolism-related and core clock gene expression in the cactus *Opuntia ficus-indica*. *Plant Physiology* 156: 1978–1989.

McCormick RF, Truong SK, Sreedasyam A, Jenkins J, Shu S, Sims D, Kennedy M, Amirehahimi M, Weers BD, McKinley B et al. 2018. The Sorghum bicolor reference genome: improved assembly, gene annotations, a transcriptome atlas, and signatures of genome organization. *The Plant Journal* 93: 338–354.

McKain MR, McNeal JR, Kellar PR, Egliarte LE, Pires JC, Leebens-Mack J. 2016. Timing of rapid diversification and convergent origins of active pollination within Agavoideae (Asparagaceae). *American Journal of Botany* 103: 1717–1729.

Michael TP, Mockler TC, Breton G, McEntee C, Byer A, Trout JD, Hazen SP, Shen R, Priest HD, Sullivan CM et al. 2008. Network discovery pipeline elucidates conserved time-of-day-specific cis-regulatory modules. *PLoS Genetics* 4: e14.

Ming R, VanBuren R, Wai CM, Tang H, Schatz MC, Bowers JE, Lyons E, Wang M-L, Chen J, Biggers E et al. 2015. The pineapple genome and the evolution of CAM photosynthesis. *Nature Genetics* 47: 1435–1442.

Minh BQ, Schmidt HA, Chernomor O, Schrempf D, Woodhams MD, von Haeseler A, Lanfear R. 2020. IQ-TREE 2: new models and efficient methods for phylogenetic inference in the genomic era. *Molecular Biology and Evolution* 37: 1530–1534.

Moseley RC, Mewalal R, Motta F, Tuskan GA, Haase S, Yang X. 2018. Conservation and diversification of circadian rhythmicity between a model Crassulacean acid metabolism plant *Kalanchoe fedtschenkoi* and a model C₃ photosynthesis plant *Arabidopsis thaliana*. *Frontiers in Plant Science* 9: 1757.

Nguyen L-T, Schmidt HA, von Haeseler A, Minh BQ. 2015. IQ-TREE: a fast and effective stochastic algorithm for estimating maximum-likelihood phylogenies. *Molecular Biology and Evolution* 32: 268–274.

Nueda MJ, Tarazona S, Conesa A. 2014. Next maSigPRO: updating maSigPRO bioconductor package for RNA-seq time series. *Bioinformatics* 30: 2598–2602.

O'Leary B, Park J, Plaxton WC. 2011. The remarkable diversity of plant PEPC (phosphoenolpyruvate carboxylase): recent insights into the physiological functions and post-translational controls of non-photosynthetic PEPCs. *Biochemical Journal* 436: 15–34.

O'Leary B, Rao SK, Kim J, Plaxton WC. 2009. Bacterial-type phosphoenolpyruvate carboxylase (PEPC) functions as a catalytic and regulatory subunit of the novel class-2 PEPC complex of vascular plants. *The Journal of Biological Chemistry* 284: 24797–24805.

Ouyang S, Zhu W, Hamilton J, Lin H, Campbell M, Childs K, Thibaud-Nissen F, Malek RL, Lee Y, Zheng L et al. 2007. The TIGR rice genome annotation resource: improvements and new features. *Nucleic Acids Research* 35: D883–D887.

R Core Team. 2021. *R: a language and environment for statistical computing*. Vienna, Austria: R Foundation for Statistical Computing.

Robinson MD, McCarthy DJ, Smyth GK. 2010. EDGER: a Bioconductor package for differential expression analysis of digital gene expression data. *Bioinformatics* 26: 139–140.

Rosnow JJ, Edwards GE, Roalson EH. 2014. Positive selection of Kranz and non-Kranz C₄ phosphoenolpyruvate carboxylase amino acids in Suaedoideae (Chenopodiaceae). *Journal of Experimental Botany* 65: 3595–3607.

Sheehan H, Feng T, Walker-Hale N, Lopez-Nieves S, Pucker B, Guo R, Yim WC, Badgami R, Timoneda A, Zhao L et al. 2020. Evolution of l-DOPA 4,5-dioxygenase activity allows for recurrent specialisation to betalain pigmentation in Caryophyllales. *The New Phytologist* 227: 914–929.

Silvera K, Winter K, Rodriguez BL, Albion RL, Cushman JC. 2014. Multiple isoforms of phosphoenolpyruvate carboxylase in the Orchidaceae (subtribe Oncidiinae): implications for the evolution of Crassulacean acid metabolism. *Journal of Experimental Botany* 65: 3623–3636.

Smith SD, Hartsock TL, Nobel PS. 1983. Ecophysiology of *Yucca brevifolia*, an arborescent monocot of the Mojave desert. *Oecologia* 60: 10–17.

Streisfeld MA, Rausher MD. 2009. Genetic changes contributing to the parallel evolution of red floral pigmentation among *Ipomoea* species. *The New Phytologist* 183: 751–763.

Suyama M, Torrents D, Bork P. 2006. PAL2NAL: robust conversion of protein sequence alignments into the corresponding codon alignments. *Nucleic Acids Research* 34: W609–W612.

Tabi T, Patil S, Chollet R, Cushman JC. 2000. A minimal serine/threonine protein kinase circadianly regulates phosphoenolpyruvate carboxylase activity in crassulacean acid metabolism-induced leaves of the common ice plant. *Plant Physiology* 123: 1471–1482.

Wai CM, VanBuren R. 2018. Circadian regulation of pineapple CAM photosynthesis. In: Ming R, ed. *Genetics and genomics of pineapple*. Cham, Switzerland: Springer International Publishing, 247–258.

Wai CM, Weise SE, Ozersky P, Mockler TC, Michael TP, VanBuren R. 2019. Time of day and network reprogramming during drought induced CAM photosynthesis in *Sedum album*. *PLoS Genetics* 15: e1008209.

Wang F, Liu R, Wu G, Lang C, Chen J, Shi C. 2012. Specific downregulation of the bacterial-type PEPC gene by artificial microRNA improves salt tolerance in *Arabidopsis*. *Plant Molecular Biology Reporter* 30: 1080–1087.

Wickell D, Kuo L-Y, Yang HP, Ashok AD, Irisarri I, Dadras A, de Vries S, de Vries J, Huang Y-M, Li A et al. 2021. Underwater CAM photosynthesis elucidated by *Isoetes* genome. *Nature Communications* 12: 6348.

Winter K, Holtum JAM, Smith JAC. 2015. Crassulacean acid metabolism: a continuous or discrete trait? *The New Phytologist* 208: 73–78.

Wong WSW, Yang Z, Goldman N, Nielsen R. 2004. Accuracy and power of statistical methods for detecting adaptive evolution in protein coding sequences and for identifying positively selected sites. *Genetics* 168: 1041–1051.

Wu G, Anafi RC, Hughes ME, Kornacker K, Hogenesch JB. 2016. METACYCLE: an integrated R package to evaluate periodicity in large scale data. *Bioinformatics* 32: 3351–3353.

Yang X, Hu R, Yin H, Jenkins J, Shu S, Tang H, Liu D, Weighill DA, Cheol Yim W, Ha J et al. 2017. The *Kalanchoe* genome provides insights into convergent evolution and building blocks of Crassulacean acid metabolism. *Nature Communications* 8: 1899.

Yang Z. 2007. PAML 4: phylogenetic analysis by maximum likelihood. *Molecular Biology and Evolution* 24: 1586–1591.

Yin H, Guo H-B, Weston DJ, Borland AM, Ranjan P, Abraham PE, Jawdy SS, Wachira J, Tuskan GA, Tschaplinski TJ et al. 2018. Diel rewiring and positive selection of ancient plant proteins enabled evolution of CAM photosynthesis in *Agave*. *BMC Genomics* 19: 588.

Supporting Information

Additional Supporting Information may be found online in the Supporting Information section at the end of the article.

Table S1 Soil moisture values for species included here under well watered and drought conditions.

Table S2 Raw Li-Cor data for *Hesperaloe parviflora*, *Hesperaloe nocturna* and *Hosta venusta*.

Table S3 Titratable acidity measurements for *Hesperaloe parviflora*, *Hesperaloe nocturna* and *Hosta venusta*.

Table S4 Gene families with time-structured expression across all eight species.

Table S5 Gene families with time-structured expression in all species but *Hosta venusta*.

Table S6 Analysis of circadian-annotated genes in METACYCLE, using all species except Agave and Beschorneria, which had too few replicates and time points after data cleaning.

Table S7 Abbreviated ANOVA results of testing effect of species on phase of gene expression.

Please note: Wiley Blackwell are not responsible for the content or functionality of any Supporting Information supplied by the authors. Any queries (other than missing material) should be directed to the *New Phytologist* Central Office.